



Contents lists available at SciVerse ScienceDirect

Surface & Coatings Technology

journal homepage: www.elsevier.com/locate/surfcoat

Atmospheric pressure PECVD based on a linearly extended DC arc for adhesion promotion applications

Liliana Kotte^{a,*}, Holger Althues^a, Gerrit Mäder^a, Julius Roch^a, Stefan Kaskel^a, Ines Dani^a, Tobias Mertens^b, Franz J. Gammel^b

^a Fraunhofer IWS, Winterbergstrasse 28, Dresden, Germany

^b EADS Deutschland GmbH, Innovation Works Germany, Dept. IW-MS, 81663 Munich, Germany

ARTICLE INFO

Available online xxxx

Keywords:

Atmospheric pressure PECVD
Atmospheric pressure plasma
Plasma surface treatment
Silicon dioxide films
Adhesion layers

ABSTRACT

In the aircraft industry, an increasing demand for adhesion promotion layers for titanium based materials is observed to replace polluting and unhealthy substances. Plasma enhanced chemical vapour deposition (PECVD) at atmospheric pressure (AP) seems to be favourable for the deposition of thin silica-like layers. In this work, a linearly extended and scalable DC arc plasma source is used for PECVD of silica layers on Ti₆Al₄V. The influence of the precursor chemistry is evaluated for HMDSO and TEOS precursors. Using HMDSO, hydrophobic almost stoichiometric SiO₂ coatings with a carbon content of 3 at.-% to 5 at.-% are deposited on the titanium alloy substrate. For TEOS, hydrophilic carbon-free stoichiometric SiO₂ coatings are deposited. The dynamic deposition rate for TEOS is 3 times lower than that for HMDSO (up to 640 nm³/min). For the intended coating of slightly curved substrates, the film properties and deposition rates are studied for different working distances from 20 mm up to 60 mm. For 60 mm the deposition rate is reduced by a factor 6 compared to 20 mm, also the index of refraction of the film decreases from 1.45 at 20 mm distance to 1.39 at 60 mm. With increasing distance, the particle size and concentration on the surface increases and leads to less dense structures than in the case of shorter distances.

The wedge test is used to evaluate the adhesion properties of the layer. The HMDSO-based coatings exhibit a good long-term durability and a high bonding strength comparable to that of the currently used standard pre-treatment, but without the use of harmful substances.

© 2013 Elsevier B.V. All rights reserved.

1. Introduction

Plasma treatment at atmospheric pressure is broadly used for surface modification of various materials [1–3]. It has been established to remove organic residues like grease and oil from surfaces and to activate the surface by varying the surface energy of the material. A further application is the deposition of nanometer-thin silicon dioxide adhesion layers, improving bonds between the used glue and light metal or stainless steel [4,5]. The conformal coating of shaped or embossed substrates with working distances of up to 60 mm is increasingly important for an improved, economical and environmental friendly corrosion protection. Furthermore it promotes the adhesion for bonds of light-weight materials in aircraft and automobile industry. Further specifications of this adhesion layer are an increased long-term durability of the adhesive bond and the resistance against environmental influences such as temperature and humidity. The aim of applying adhesion layers is to reduce, respectively to replace, the presently necessary risky handwork with aggressive chemicals. To answer this requirement the Fraunhofer IWS offers a large-area plasma technology at atmospheric pressure [6].

This work focuses on the development of a new AP-PECVD method, using a direct current powered atmospheric pressure arc (LARGE plasma source). In the first part of the paper, the working principle of the innovative LARGE plasma source and the coating equipment is described. The second part deals with the deposition of silicon dioxide adhesion layers on a titanium alloy using an open atmospheric pressure plasma process based on the LARGE technology. The compact construction of the equipment facilitates the integration into a process line, e.g. the installation on a robot arm, for the continuous deposition of silicon dioxide films on shaped substrates of steel, light metals or light-metal alloys as well as the plasma activation of polymer or fiber reinforced plastic surfaces.

For the intended application as adhesion promotion layers, the bonding strength using an epoxy based glue is evaluated.

2. Experimental

2.1. Materials

For the investigations square specimens of the titanium alloy Ti₆Al₄V with an edge length of 150 mm and a thickness of 2.0 mm

* Corresponding author. Tel.: +49 351833913439; fax: +49 35183391330.
E-mail address: liliana.kotte@iws.fraunhofer.de (L. Kotte).

are used. In this alloy, the main elements are the α -phase-stabilizer aluminum and the β -phase-stabilizer vanadium.

For spectroscopic film characterization silicon dioxide films are deposited on polished stainless steel 1.4301 ($R_a = 60$ nm) as reference.

2.2. Linearly extended DC arc plasma source

This newly developed plasma source (based on the LARGE – long arc generator principle [7]) offers a scalable working width and operates with a range of plasma gases, flowing perpendicular to the plasma axis. The basic principle of this technology is equivalent to the conventional plasma (powder) spraying. The difference between the LARGE plasma source and an industrial plasma spraying system is the size of the treated surface area. A state of the art plasma burner has a working area of only a few square centimeters. The LARGE plasma source possesses a linearly extended and stabilized DC arc plasma with a length of up to 350 mm.

The plasma source is optimized for special requirements of atmospheric pressure PECVD applications [8]. The working width is increased from originally 150 mm to 350 mm, the process stability is improved, and the plasma homogeneity is optimized by an adapted plasma gas feeding system. The principle of the plasma source is described in Fig. 1. The arc occurs in an argon-containing atmosphere between opposite electrodes. The distance of the electrodes is essential for the working width of the plasma source and affects the required power of the DC arc. The shape of the arc is primarily determined by heat convection and consequently very instable. Therefore, the arc is stabilized by three mechanisms, shown at the right side of Fig. 2. The first one is the stabilization by cooled copper walls enclosing the arc. The relaxation of activated species and the heat loss of the plasma reduce the plasma conductivity at the transition zone. Thus, the arc uses the minimum discharge resistance and avoids the nearness of the cooled copper wall. Secondly, the permanent gas supply cools down the sector around the arc core. Due to the high gradient in conductivity the arc confines in the center. At last, the arc is fixed by the Lorentz force acting on the charge carriers in the arc. This creates a momentum against the down-streaming plasma gas. The stabilization allows the arc to burn between the two electrodes in a linear direction. Additionally, the electrical resistance of the surrounding copper walls must be higher than that of the direct arc. This is achieved by electrically cascading the walls, i.e. by ceramic isolation plates in between the copper plates [9].

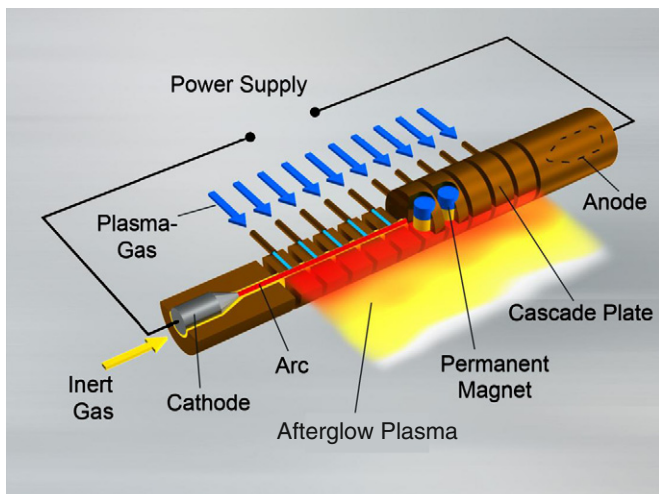


Fig. 1. Principle of the linearly extended DC arc (LARGE).

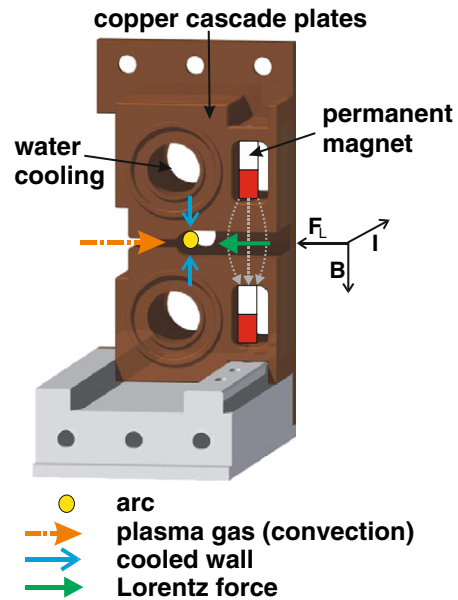


Fig. 2. Mechanisms of the arc stabilization.

With this construction it is possible to enable nearly any arc length; the maximum reached arc length in the laboratory is 350 mm.

2.3. Equipment for PECVD and process development

For PECVD and plasma-chemical etching [10], a remote gas feeding system is installed in front of the plasma source to prevent contaminations in the plasma source. For the deposition of silicon dioxide layers a feeding system made from hard anodized AlMg31 and exhibiting discrete round nozzles is used (Fig. 3). The equipment is cooled by deionized water. The gaseous precursor is distributed via cascaded volumes to ten afterglow plasma nozzles, into which the precursor is injected by two drillings with a diameter of 1 mm respectively at 60° angle. The two drillings are placed on opposite sides of the nozzle and thus are optimized to mix with the afterglow plasma. Round nozzles allow a reduction of the cross-sectional area of the afterglow plasma by four times compared to an operation without gas feeding system, resulting in a higher gas velocity of up to 80 m/s [11]. Thus, the energy of the afterglow plasma is still high enough for the dissociation of the precursor. The remote gas flow determines its

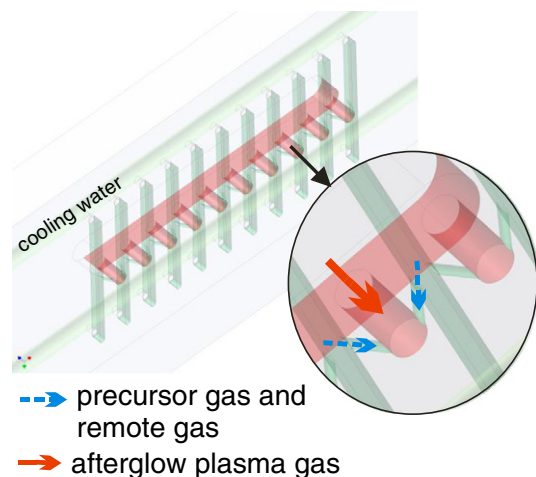


Fig. 3. Design of the remote gas feeding system for film deposition.

mixing with the afterglow plasma. Corresponding to fluid-dynamic simulations (FLUENT) the ratio between plasma gas and remote gas flow should be equal or higher than 2:1. This value was confirmed by previous experiments. At ratios lower than 2:1 turbulences in the plasma gas flow disturb the arc stability.

The substrate is moved in front of the plasma source at a distance from 20 mm up to 60 mm. The maximum substrate width is defined by the arc length being 150 mm for the presented experiments. For the deposition of silicon dioxide the precursors hexamethyldisiloxane (HMDSO, $C_6H_{18}OSi_2$, cas no. [107-46-0]) and tetraethylorthosilicate (TEOS, $(C_2H_5O)_4Si$, cas no. [78-10-4]) are used. The precursors are heated up to 80 °C and 110 °C, resp. For a better comparison of the deposition rate, some experiments are carried out at a temperature of 60 °C for TEOS. For 60 °C and 110 °C, resp., both precursors have the same vapour pressure of about 16.4 kPa. A mixture of argon and the precursor, diluted by nitrogen and oxygen, is added into the afterglow plasma. The remote gas line has to be heated up to 110 °C, to avoid the condensation of the precursor. Table 1 summarizes the main process parameters for the silicon dioxide deposition.

2.4. Film characterization

The silicon dioxide films, deposited by the atmospheric pressure PECVD process, are analysed by Fourier transform infrared (FTIR) spectroscopy, spectro-ellipsometry, and SEM. For a precise film characterization, the films are deposited on polished stainless steel ($R_a = 60$ nm).

The ellipsometric measurements (VASE, J. A. Woollam) are performed in the wavelength range between 350 nm and 1050 nm with the incidence angles of 65°, 70°, and 75°. For analysis, the silica films are modelled by a compact film covered by a top rough film with voids. The compact silicon dioxide film directly grows on the substrate surface and is described by a Cauchy model. The subsequent top layer is fitted by an effective medium approximation layer (EMA, Bruggeman), consisting of 50% silicon dioxide (optical constants of the compact layer) mixed with 50% spherical voids.

The chemical composition of the films is analysed by FTIR reflection spectroscopy using IRspecXL® for large substrates of up to 30 cm × 30 cm. The FTIR reflection spectra are measured at an incidence angle of 73° with p-polarised light between 6000 m^{-1} and 400 cm^{-1} .

Representative samples are furthermore analysed by XPS using a Quantum 2000 spectrophotometer (Physical Electronics) equipped with an Al K α (1486.6 eV) monochromatic source at base pressures less than 10^{-6} Pa with a 45° take-off angle. The spectra are obtained using a spot size of 200 μm . For the survey spectra a pass energy of 117.4 eV is used, for high-resolution spectra the pass energy is 11.75 eV. High-resolution spectra are charge-compensated by setting the binding energy of the C1s peak to 284.8 eV. Peaks are fitted (Gaussian/Lorentzian curves) after background subtraction (Shirley type) by using the MultiPak 8.2 software. For quantification of the survey spectra the peak area of the spectra is calculated after background subtraction by integration and multiplication by sensitivity factors according to Moulder [12]. Subsequently, the results are normalised to 100 at.-%. Depth measurements are carried out by

Table 1

Process parameter.

Plasma gases	80–140 slm Ar + 50–80 slm N ₂
Remote (dilution) gases	50–70 slm N ₂ + 15–30 slm O ₂
Precursors	HMDSO, TEOS
Working distance	20 to 60 mm
Working width	150 mm
Power	15–25 kW
Deposition atmosphere	ambient air
Substrate velocity	7.5 and 9 m/min

using 2 keV Argon sputtering with a sputtering rate of 120 nm/min or 7 nm/min (calibrated on SiO₂).

2.5. Bonding and wedge test method

The wedge test according to the German standard DIN 65448 is an application specific test to evaluate structural glues for the aircraft and astronautics industry performed by EADS (a detailed description of sample preparation and analysis as well as reference samples is presented in [13]). The test is carried out in a climate chamber at 95% relative humidity and 50 °C. The initial crack length and the crack propagation are measured. The rate at which the crack grows is microscopically monitored. In this paper we test silicon dioxide (from HMDSO) films on Ti₆Al₄V substrates, bonded with epoxy based adhesive FM 73 M (cured at 120 °C for 90 min in an autoclave at a pressure of 0.25 MPa). The Matrix of the FM 73 M is DGEBA (diglycidylether of bisphenol-A) with the hardening component 2,4-tolyl-1,1-dimethylurea.

The samples (100 × 200 × 2 mm³) are cleaned (almeco 18, Henkel AG Co. KGaA, at 70 °C for 15 min) and textured (alkaline etched with Turco 5578, Henkel AG Co. KGaA, at 95° for 5 min). The silicon dioxide films are evaluated against the industrial standard film produced by anodization (NaTESi). Here the titanium alloy surface is anodized by an electrolyte (sodium hydroxide (NaOH), sodium tartrate (Na₂C₄H₄O₆), ethylenediaminetetraacetic acid (EDTA) and sodium silicate (Na₂SiO₃)) and subsequently bonded. However, the NaTESi process is no longer applicable due to environmental and health concerns.

3. Results and discussion

In the first part of the work, the influence of the precursor chemistry on the film properties is studied. Two typical FTIR spectra of the deposited films are presented in Fig. 4, showing that TEOS generates hydroxylated silica films (SiO₂:OH), whereas HMDSO forms films containing the precursor's carbon (SiO_xC_y:OH). FTIR spectra of the films show the typical Si–CH₃ bonds at 1260 cm^{-1} . XPS analysis validated 3 at.-% to 5 at.-% carbon in the film [13].

The different oxygen amount in the precursor itself may be responsible for the fact that HMDSO is not able to oxidize the carbon into volatile CO₂.

All films exhibit a high concentration of OH groups resulting from the precursor itself and from the open deposition atmosphere with a relative humidity of approximately 30%. The surrounding atmosphere is partly blended into the afterglow plasma flow and is subsequently dissociated. The hydroxyl groups are evenly distributed in the film and can not be removed by a following heat treatment.

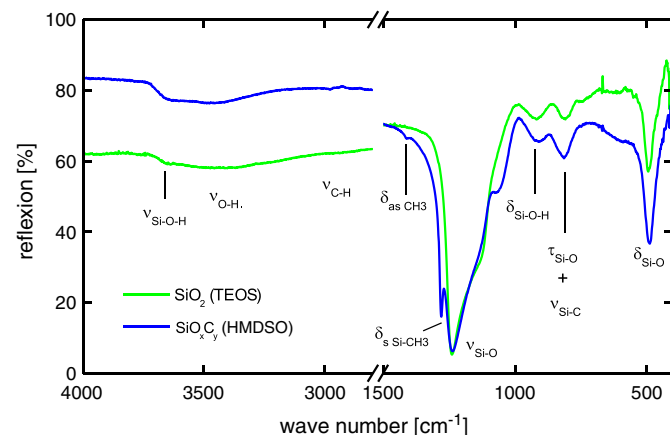


Fig. 4. FTIR spectra of SiO₂ films deposited with the precursors HMDSO and TEOS on polished stainless steel.

Wetting measurements with the lying drop method show a water contact angle of between 24° and 37° for silicon dioxide films from TEOS. This confirms the distribution of the hydroxyl groups in the film. SiO_xC_y films from HMDSO show water contact angles greater than 86°. The carbon in the film is bonded in $\text{Si}-\text{CH}_3$, in combination with the remaining $\text{Si}-\text{OH}$ fragments a more hydrophobic surface than for TEOS is created. The wettability is influenced by the organic concentration in the silicon dioxide films [11,15].

The precursor chemistry also influences the deposition rate. Fig. 5 presents the dynamic deposition rate versus the nitrogen concentration in the plasma gas flow (180 slm total). The dynamic deposition rate is the product of film thickness and the substrate velocity divided by the number of cycles. The precursor concentration in the remote gas flow is constant in this experiment. Therefore, the precursors are heated up to 60 °C for HMDSO and 110 °C for TEOS. For these temperatures both precursors have a vapour pressure of 16,4 kPa. The gas flows for HMDSO based films are 50 slm N_2 , 20 slm O_2 , and 0,8 slm Ar bubbled through HMDOS as remote gas. For the TEOS based films the process parameters are 25 slm N_2 , 25 slm O_2 and 1 slm Ar bubbled through TEOS as remote gas.

For HMDSO, increasing the nitrogen concentration in the plasma gas results in an increase of the deposition rate from 350 nm²/min up to 470 nm²/min. For TEOS the dynamic deposition rate is nearly constant at 100 nm²/min.

The generally lower deposition rate for TEOS may be explained by the presence of only one Si atom in the TEOS molecule compared to 2 in HMDSO. As nitrogen is regarded as the energy carrier in this PECVD process [14], with increasing nitrogen concentration an increased dynamic deposition rate is expected for both precursors. Apparently, even the higher energy in the nitrogen rich plasma is not sufficient to dissociate more Si–O bonds in the TEOS molecules.

The second part of the study deals with the influence of the working distance on the film properties and deposition rate. In Fig. 6 the dynamic deposition rate for the HMDSO precursor in dependence on the distance between plasma source and substrate is shown for a varied nitrogen flow in the plasma gas. At a working distance of 20 mm a film with a dynamic deposition rate of approximately 640 nm²/min is deposited. By doubling the distance the deposition rate is three times reduced. At a distance of 60 mm, the rate decreases to 120 nm²/min. For a distance of 20 mm, dense silicon dioxide films with an index of refraction n of 1.45 (at 550 nm) are deposited (Fig. 6). For the largest distance of 60 mm the index of refraction decreases to 1.39. The concentration of the precursor in the afterglow plasma decreases with larger distances due to reactions of the precursor fragments with each other as well as with atmospheric species.

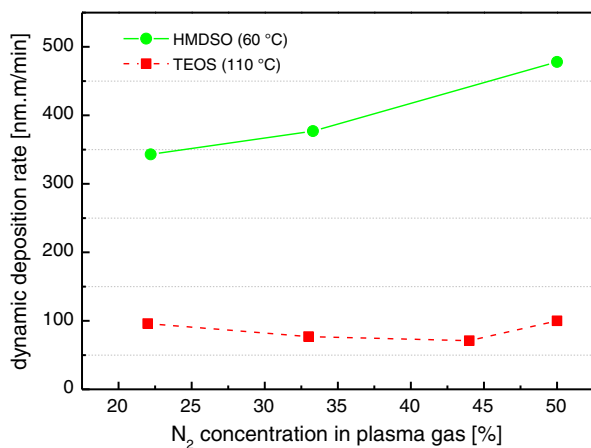


Fig. 5. Comparison of the dynamic deposition rate of TEOS and HMDSO in dependence on nitrogen concentration in the plasma gas flow; PECVD constant process parameter: 7,5 m/min substrate velocity, working distance 20 mm, substrate polished stainless steel.

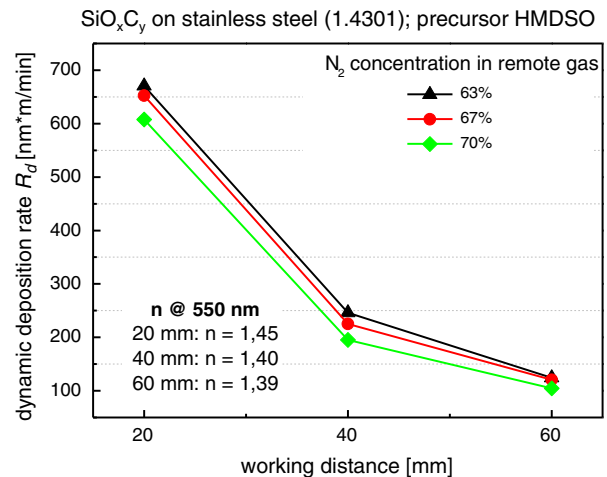


Fig. 6. dynamic deposition rate of SiO_xC_y (HMDSO) film deposition depending on working distances; process parameter: 100 slm Ar + 60 slm N_2 plasma gas, 30 slm O_2 + (50–70) slm N_2 remote gas.

Agglomerates in the gas phase will be generated at a critical distance and can also be deposited on the substrate. The energy of the afterglow plasma exponentially decreases with the increase of the working distance, caused by recombination of active species. This explanation is confirmed by an analysis of the film morphology, also affected by the working distance. Fig. 7 presents SEM pictures of $\text{Ti}_6\text{Al}_4\text{V}$ substrates covered by an approximately 150 nm thick SiO_xC_y film deposited for different distances. Cryo fracture SEM pictures confirm, that the silicon dioxide films are compact and dense [13]. With increasing distance, the particle density on the surface will rise as well. The partially agglomerated particles are formed in the gas phase and. These particles are deposited on the surface and can be embedded in the deposition cycle.

For the intended application as adhesion promotion layers, two 25 mm wide coated titanium alloy surfaces are bonded with epoxy based glue FM 73 M and cured at 120 °C for 90 min in an autoclave at a pressure of 0.25 MPa. To ensure a penetration of the adhesive in an open porous morphology a vacuum is helpful. Using autoclave technology both aspects could be combined. Also oxygen inclusions in the bondline could be avoided with using autoclave technology. The autoclave processes are standard in aerospace industry for structural bonding.

Both films prepared from TEOS and HMDSO are analysed. The deposition parameters can be seen in Fig. 8. The surface morphology of the HMDSO based film is similar to that one presented in Fig. 7a. A compact SiO_xC_y film with globular particles is deposited. For thicker films the higher concentration of particles and agglomerates looks like a cauliflower surface. The adhesion of the titanium alloy to the glue is based on a hydrogen bridge bond and on a covalent bonding between the SiO_xC_y films and glue [13]. The bonds are evaluated using a wedge test. Here a wedge is positioned in between the bonded titanium alloy strips to stress the test piece. The test is carried out in a conditioning chamber at 95% relative humidity and 50 °C. The crack growth is measured at defined times and is proven by a microscope. Subsequently, the samples are damaged for a local crack analysis. The results are presented in Fig. 8. The adhesion force of the titanium alloy bonding depends on the morphology of the surface and the chemistry. The particles and agglomerates on the surface enlarge the effective surface and offer a better mechanical anchoring for the glue. The aim is to achieve a long term stability comparable to that of the NaTESi preparation. Very good long term durability results are achieved for the 100 nm thick HMDSO based film deposited at a distance of 20 mm. For deposition of this film, the temperature of the precursor HMDSO is 80 °C. The carrier gas Ar (0.5 slm) is bubbled

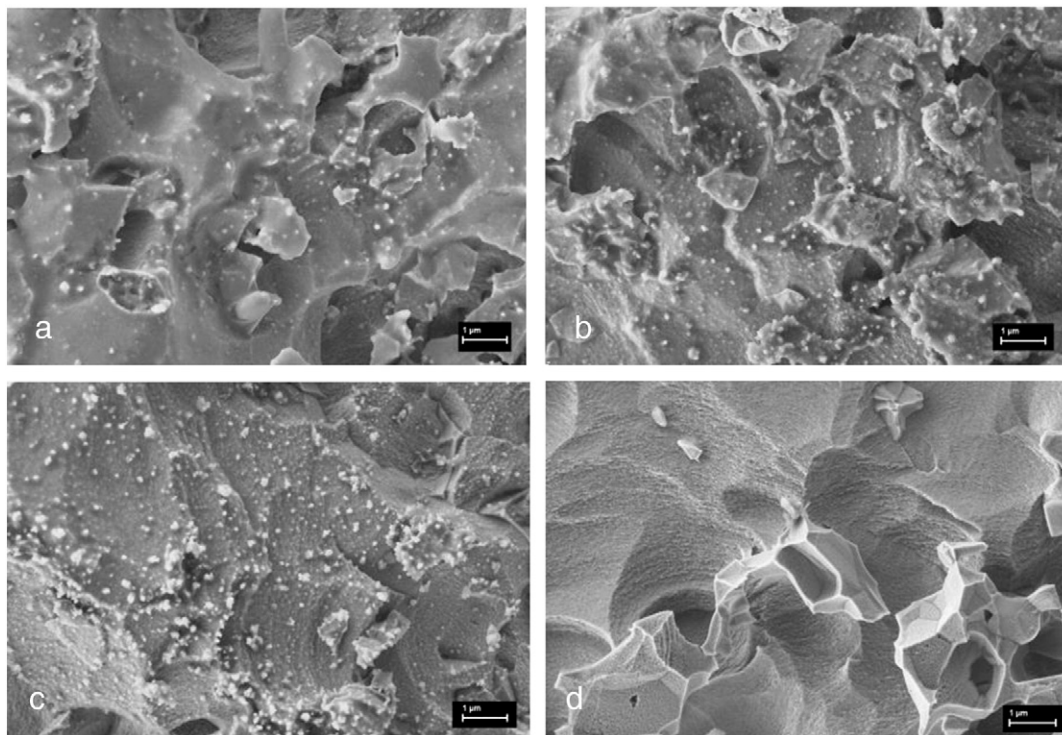


Fig. 7. SEM pictures of $\text{Ti}_6\text{Al}_4\text{V}$ coated with ca. 150 nm SiO_xC_y film deposited at a) 20 mm, b) 40 mm, c) 70 mm working distance and d) reference.

through the HMDSO and is mixed with 50 slm N_2 and 30 slm O_2 . This remote gas mixture flows into the plasma gas (100 slm Ar and 60 slm N_2). One cycle with a substrate velocity of 9 m/min is carried out for an approximately 100 nm thick silica film. The test results of the films are comparable with the crack length of NaTESi pre-treated titanium alloy surfaces. Independent from the pre-treatment (Turco 5578 and Turco 5578 plus bond primer), this film reaches the requested specification. All treatments lead to a comparable initial crack length and bonding strength, respectively. The initial crack length is between 24 and 28 mm for all treatments. Due to this, for all joints the initial failure loci are similar. The failure is initiated in a cohesive manner in the middle of the adhesive. After the introduction of the joints

into the climate chamber the failure is transferred within 75 min close to the titanium surface.

The adhesion results of the plasma treated samples (crack growth of 45–50 mm) are slightly inferior to the NaTESi reference with 40 mm crack growth, but clearly better than the industrially available treatment Turco 5578 with 70 mm. The joints treated with Turco 5578 show a crack length of $72.8 \text{ mm} \pm 4.3 \text{ mm}$.

4. Conclusions

The atmospheric pressure PECVD of silicon dioxide adhesion layers on a titanium alloy is successfully demonstrated. The precursor chemistry determines the composition of the film as well as the deposition rate. The energy of the afterglow plasma is sufficient for the dissociation of both HMDSO and TEOS precursors. With HMDSO dense and quasi stoichiometric silicon dioxide films with methyl and hydroxyl groups are deposited. TEOS forms carbon-free dense and compact hydroxylated silicon dioxide films. The chemical composition of the films determines the wetting behaviour. Silicon dioxide films with carbon (generated with HMDSO) are hydrophobic. TEOS-based silicon dioxide films without carbon are hydrophilic. The morphology of the films depends on the working distance, the precursor concentration, the remote gas flow and composition. In dependence of the deposition parameters, the silicon dioxide films show surface morphologies from a dense even surface up to globular and cauliflower structures in the top layer.

Application specific adhesion tests confirm the potential of the films for the adhesion layer. The results of the wedge test (DIN 65448) exhibit very promising long term stabilities of the SiO_xC_y films on titanium alloy. The crack length is comparable to that of the presently used pre-treatment NaTESi, which has to be replaced in the future. The LARGE-PECVD technology in an open atmosphere provides a very suitable method to deposit silicon dioxide adhesion layers on shaped substrates. To get more flexibility for the processing of large shaped parts, the LARGE plasma source with its coating system will be installed on a robot arm in near future.

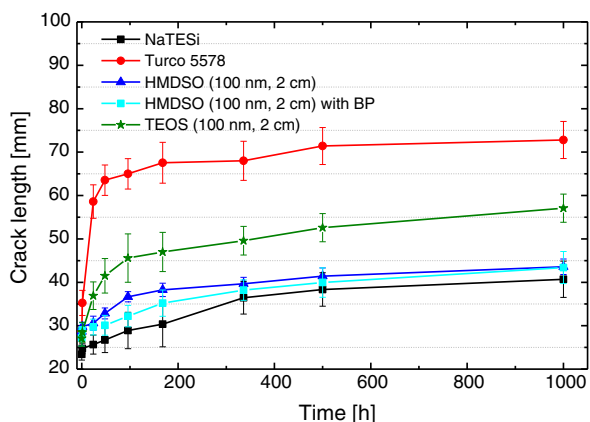


Fig. 8. Crack propagation of coated and pre-treated $\text{Ti}_6\text{Al}_4\text{V}$ samples in the wedge test (average of five specimens); constant PECVD deposition process parameter for both precursors: 2 cm working distance, 9 m/min substrate velocity, 100 slm Ar + 60 slm N_2 as plasma gas, 70 A arc current, 45° tilting angle of plasma source, process parameter for deposition with TEOS: precursor temperature 60°C , bubble with 2.2 slm Ar carrier gas, 25 slm N_2 + 25 slm N_2 as remote gas, 10 cycle for an approximately 100 nm silica film.

Acknowledgement

Financial support of the EC (FP7 framework, N2P – Nano to Production) is gratefully acknowledged.

References

- [1] C. Tendero, C. Tixier, P. Tristant, J. Desmaison, P. Leprince, *Spectrochim. Acta Part B* 61 (2006) 2–30.
- [2] A. Villermet, P. Cocolios, G. Rames-Langlade, F. Coeuret, J.L. Gelot, E. Prinz, F. Förster, *Surf. Coat. Technol.* 174–175 (2003) 899–901.
- [3] M. Noeske, J. Degenhardt, S. Strudthoff, U. Lommatzsch, *Int. J. Adhes. Adhes.* 24 (2004) 171–177.
- [4] A. Pfuch, K. Horn, J. Schmidt, M. Günther, A. Heft, A. Schimanski, *Galvanotechnik* 12 (2010) 2884–2889.
- [5] M. Akram, K.M.B. Jansen, L.J. Ernst, S. Bhowmik, *Int. J. Adhes. Adhes.* 31 (2011) 598–604.
- [6] Patent EP 97870823 (1997).
- [7] R. Hartmann, G. Kraut, K. Landes, *Eur. Phys. J. Appl. Phys.* 8 (1999) 253.
- [8] V. Hopfe, D. Rogler, G. Mäder, I. Dani, K. Landes, E. Theophile, M. Dzulko, C. Rohrer, C. Reichhold, *Chem. Vap. Deposition* 11 (2005) 510–522.
- [9] P. Grabau, *Elektrische Diagnose einer Long-Arc-Plasmaquelle zur Erhöhung der Prozesssicherheit und –zuverlässigkeit*, (diploma thesis) Technische Universität Dresden, 2007.
- [10] D. Linaschke, M. Leistner, P. Grabau, G. Mäder, W. Grähler, I. Dani, S. Kaskel, E. Beyer, *IEEE Trans. Plasma Sci.* 37 (6) (2009) 979–984.
- [11] L. Kotte, *Jahrbuch Oberflächentechnik*, Band 68, Leuze Verlag, Bad Saulgau, 2012.
- [12] J.F. Moulder, J. Chastain, W.F. Stickle, et al., *Handbook of x-ray photoelectron spectroscopy: a reference book of standard spectra for identification and interpretation of XPS data*, Physical Electronics, 1995.
- [13] T. Mertens, F.J. Gammel, M. Kolb, O. Rohr, L. Kotte, S. Tschöcke, S. Kaskel, U. Krupp, *Int. J. Adhes. Adhes.* 34 (2012) 46–54.
- [14] G. Mäder, *Atmosphärendruck-Plasma-Beschichtungsreaktoren*, (PhD thesis) Fraunhofer-IRB Verlag, Stuttgart, 2008.
- [15] R. Morent, N. De Geyter, S. Van Vlierbergh, P. Duburel, C. Leys, E. Schacht, *Surf. Coat. Technol.* 203 (2009) 1366–1372.